Geoexploration
Elsevier Publishing Company, Amsterdam – Printed in The Netherlands

MAGNETOSTATIC ANOMALIES OF DIPPING PRISMS

SVEN-ERIK HJELT

*Finnish Academy, Research Council for Technical Sciences, Helsinki (Finland)**

(Accepted for publication June 9, 1972)

ABSTRACT

Hjelt, S.-E., 1972. Magnetostatic anomalies of dipping prisms. *Geoexploration*, 10:239–254.

The expressions of the magnetic field of a homogeneously magnetized, dipping prism are given. The expressions are only slightly more complicated than the corresponding formulae of vertical prisms.

The calculated examples show that the effect of finite strike length on magnetic profiles is very complex. Even for profiles perpendicular to the strike and for the maxima of these profiles no simple description of strike length effects can be given.

The expressions should prove valuable in computer interpretation of three-dimensional anomalies.

INTRODUCTION

Two popular magnetic interpretational models are the inclined dyke or thick plate and the vertical prism. The fields of dykes have been extensively discussed by Gay (1963). Fields of vertical prisms have early been calculated numerically by Vacquier et al. (1951). Formulae of an infinitely deep prism were given in a closed form by Bhattacharyya (1964). The case of finite depth extent has been considered by Sharma (1966) and Andreasen and Zietz (1969).

This article combines both models and presents the formulae of a finite, homogeneously magnetized prism with two dipping surfaces and horizontal upper surface. This new model will be called the *inclined* or *dipping prism*. The new formulae need at most some ten percent longer computing times than the vertical prism formulae.

DERIVATION OF THE FORMULAE

We make the following assumptions: (1) the magnetization is homogeneous throughout the prism; (2) demagnetization effects are neglected; (3) the prism has horizontal upper and lower surfaces; (4) the prism has vertical end surfaces (perpendicular to the strike).

We make use of the notations introduced by Sharma (1966) and define a rectangular coordinate system as follows (see Fig. 1): the z-axis is positive downwards, the y-axis

* Present address of author: c/o Outokumpu Co., Exploration Department, Tapiola, Finland.

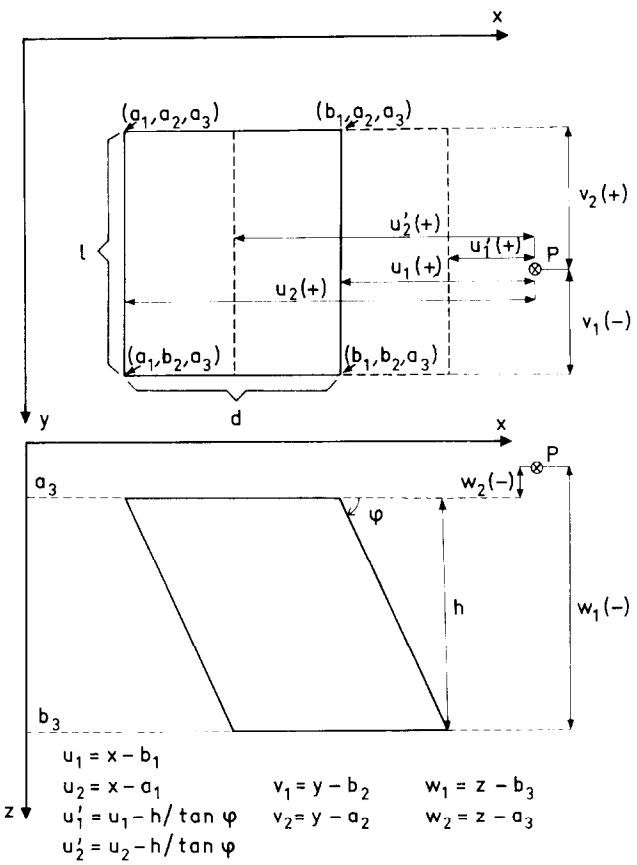

Fig. 1. The inclined prism, coordinate system and notations.

points in the strike direction and the x-axis is horizontal, perpendicular to the strike. The dipping surfaces of the prism make the angle ϕ with the positive x-axis.

The coordinates of the corner points of the prism are denoted by a_1, a_2, a_3 and b_1, b_2, b_3, where the indices refer to the x, y and z-coordinates respectively. The letter 'a' refers to a point nearer to the origin, the letter 'b' to a point more distant from the origin (see Fig. 1). At the lower surfaces of the prism ($z = b_3$) the x-coordinates increase with an amount depending on the dip. We denote correspondingly:

$$a_1' = a_1 + h/\tan\phi$$

$$b_1' = b_1 + h/\tan\phi$$

The differences between the coordinates of the field point $P(x,y,z)$ and the corners of the prism are denoted with u, v and w respectively. Indices and dashes are used in the manner described above.

If $\bar{J}$ is the magnetization of the prism, the field at P outside the prism is given by:

$$\bar{H} = \nabla \int_V \bar{J} \cdot \nabla_o \frac{1}{R} dv \tag{1}$$

where $R = \sqrt{(x-x_o)^2 + (y-y_o)^2 + (z-z_o)^2}$

is the distance between the field point P and a source point (x_o, y_o, z_o) inside the prism.

Because of the homogeneous magnetization, $\bar{J}$ can be taken outside the integral, which in turn can be transformed to an integral over the surface of the prism:

$$\bar{H} = \nabla \bar{J} \circ \int_S \frac{\bar{u}_n}{R} ds \tag{2}$$

where $\bar{u}_n$ is the unit vector in the direction of the outward normal of the prism surfaces.

The rectangular components of the anomalous field are now:

$$\left.\begin{aligned} H_x &= \sum_{i=1}^{3} J_i \cdot T_{1i} \\ H_y &= \sum_{i=1}^{3} J_i \cdot T_{2i} \\ H_z &= \sum_{i=1}^{3} J_i \circ T_{3i} \end{aligned}\right| \tag{3}$$

where: $J_1 = J_x \cdot \sin\phi - J_z \cdot \cos\phi$
$J_2 = J_y$
$J_3 = J_z$

are the components of magnetization perpendicular to the prism surfaces. The total field will be given by:

$$T = H_x \cdot \cos I_o \cdot \sin\alpha_o + H_y \cdot \cos I_o \cdot \cos\alpha_o + H_z \circ \sin I_o$$

where: I_o = inclination of the geomagnetic field; α_o = azimuth of the prism strike (with reference to geomagnetic north).

The factors T_{ij} are defined in the Appendix and their final expressions are given by:

$$\left.\begin{aligned} T_{11} &= -\sin\phi \cdot \Phi_{1u} + \cos\phi \cdot \Phi_{2v} \\ T_{12} &= \sin\phi \cdot \Phi_{2w} \\ T_{13} &= \Phi_{2v} \\ T_{21} &= \Phi_{2w} \\ T_{22} &= \Phi_{1v} \\ T_{23} &= \Phi_{2u} \\ T_{31} &= \cos\phi \cdot \Phi_{1u} + \sin\phi \cdot \Phi_{2v} \\ T_{32} &= -\cos\phi \cdot \Phi_{2w} + \Phi_{2u} \\ T_{33} &= -\Phi_{1w} \end{aligned}\right| \tag{4}$$

where:

$$\Phi_{1u} = \begin{matrix} u_1 & v_1 & w_1 \\ | & | & | \\ u_2 & v_2 & w_2 \end{matrix} \arctan\left[\frac{v \cdot (u \cdot \cos\phi + w \cdot \sin\phi)}{(u \cdot \sin\phi - w \cdot \cos\phi) \cdot R_{uvw}}\right]$$

$$\Phi_{1v} = \begin{matrix} u_1 & v_1 & w_1 \\ | & | & | \\ u_2 & v_2 & w_2 \end{matrix} \arctan\left[\frac{v^2 \cdot \cos\phi - w \cdot (u \cdot \sin\phi - w \cdot \cos\phi)}{v \cdot \sin\phi \cdot R_{uvw}}\right]$$

$$\Phi_{1w} = \begin{matrix} u_1 & v_1 & w_1 \\ | & | & | \\ u_2 & v_2 & w_2 \end{matrix} \arctan\left[\frac{v \cdot u}{w \cdot R_{uvw}}\right]$$

$$\Phi_{2u} = \begin{matrix} u_1 & v_1 & w_1 \\ | & | & | \\ u_2 & v_2 & w_2 \end{matrix} \ln\left(u + R_{uvw}\right) \qquad (5)$$

$$\Phi_{2v} = \begin{matrix} u_1 & v_1 & w_1 \\ | & | & | \\ u_2 & v_2 & w_2 \end{matrix} \ln\left(v + R_{uvw}\right)$$

$$\Phi_{2w} = \begin{matrix} u_1 & v_1 & w_1 \\ | & | & | \\ u_2 & v_2 & w_2 \end{matrix} \ln\left(u \cdot \cos\phi + w \cdot \sin\phi + R_{uvw}\right)$$

$$R_{uvw} = \sqrt{u^2 + v^2 + w^2}$$

Note 1: When $w = w_1$, always use $u' = u - h \cdot \cot\phi$; when $w = w_2$, always use u only.

Note 2: The sign of each Φ is positive, whenever there is an even number of 2's in the indices of u, v, and w. ($R_{u_1 v_1 w_1}$, $R_{u_1 v_2 w_2}$, etc.)

PROPERTIES OF THE FORMULAE

Table I shows the symmetry properties of the eq. 3–5. The symmetry is considered with respect to the center point of the prism upper surface on lines which are parallel to the coordinate axes. If the field component gets the same numerical value at two symmetric points on a line parallel to the x-axis, a letter u is indicated in Table I. The letters v and w stand for the y- and z-axis symmetries respectively. The symmetry properties given in Table I are evidently physically correct.

If $\phi = 90°$, eq. 3–5 give results which are identical with the formulae of vertical prisms given earlier (Bhattacharyya, 1964 and Sharma, 1966). If one puts $v_2 = -v_1$ and takes the limit $v_1 \to \infty$, one gets expressions which with allowance for differences in notations are identical with the two-dimensional thick plate formulae (Gay, 1963).

TABLE I

Symmetry properties of dipping prism fields

ϕ (°)	α_o (°)	I_o (°)	H_x	H_y	H_z	T
$\neq 90$	90	0–180	v	–	v	v
	0	0–180	–	–	–	–
	0–180	0	–	–	–	–
	0–180	90	v	–	v	v
90	90	0–180	v	–	u, v, w	v
	0	0–180	–	u	u	u
	0–180	0	w^*	w	–	w^*
	0–180	90	v	–	u, v, w	u, v, w

* u and v also, if $\alpha_o = 90°$.

USE OF THE FORMULAE

To calculate the anomalous fields on profiles not parallel to the axes of the prism coordinate system, it is advantageous to define the profile coordinate system $x'\,y'\,z'$ as indicated in Fig. 2A and make the transformation to the xyz-system using the expressions:

$$\begin{aligned} x &= x' \cdot \cos\beta - y' \cdot \sin\beta \\ y &= x' \cdot \sin\beta + y' \cdot \cos\beta \end{aligned} \tag{6}$$

where β is the angle between the profile and the x-axis of the prism.

If the inclination of the geomagnetic field is I_o and the strike of the prism makes the angle α_o with the magnetic north (Fig. 2B), the components of the geomagnetic field T_o in the prism coordinate system are:

$$\begin{aligned} T_{ox} &= T_o \cdot \cos I_o \cdot \sin\alpha_o \\ T_{oy} &= T_o \cdot \cos I_o \cdot \cos\alpha_o \\ T_{oz} &= T_o \cdot \sin I_o \end{aligned} \tag{7}$$

If the prism has also remanent magnetization, its components are given similarly (Fig. 2C):

$$\left.\begin{aligned} T_{rx} &= T_r \cdot \cos I_r \cdot \sin(\alpha_o - \alpha_r) \\ T_{ry} &= T_r \cdot \cos I_r \cdot \cos(\alpha_o - \alpha_r) \\ T_{rz} &= T_r \cdot \sin I_r \\ T_r &= Q \cdot T_o \end{aligned}\right| \tag{8}$$

where Q is the Königsberger ratio.

The total magnetization of the prism is then given by:

$$\left.\begin{aligned} J_x &= k \cdot (T_{ox} + T_{rx}) \\ J_y &= k \cdot (T_{oy} + T_{ry}) \\ J_z &= k \cdot (T_{oz} + T_{rz}) \end{aligned}\right| \tag{9}$$

which can directly be substituted into the eq. 3–5. One could here think of an approxima-

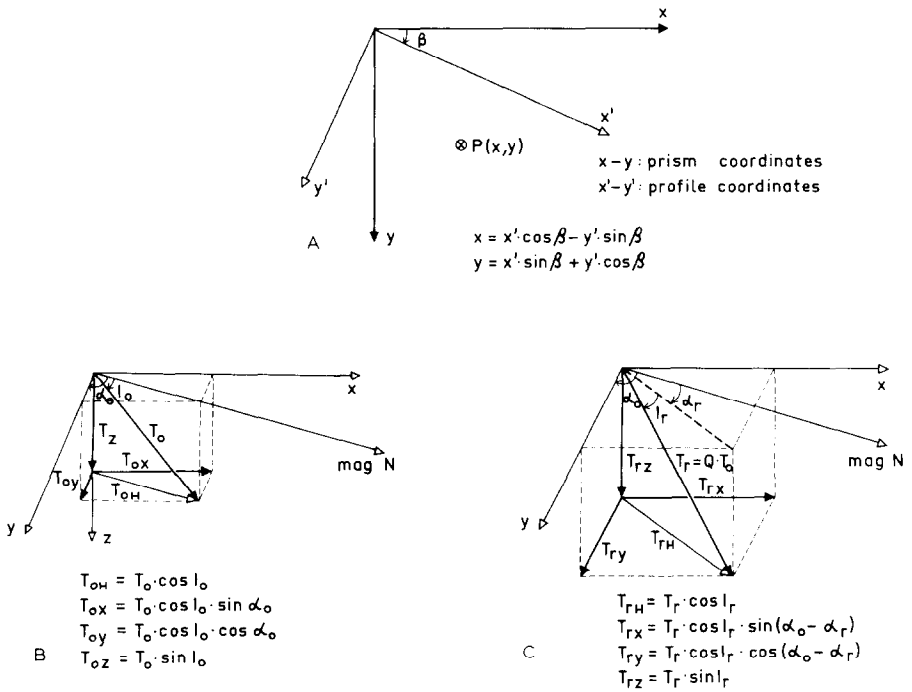

Fig. 2. The rectangular coordinate of (A) a profile, (B) the geomagnetic field and (C) the remanent magnetization.

tion of demagnetization effects by taking different values for the coefficient k in each component of $\bar{J}$.

RESULTS

The expressions have been programmed and calculations run on the IBM 360/40 computer of the Outokumpu Company. The time for calculation and print-out of a single field point was about 0,2 sec.

The effect of strike length on profiles over the center of prisms and perpendicular to the strike is shown in Fig. 3 and 4. The maximum anomaly will either decrease or increase in relation to the corresponding two-dimensional profile, depending on all parameters, but mostly on dip, the thickness/depth and strike length/thickness ratios. The changes in the maximum of the anomaly are summarized in Fig. 5 for some cases. When the prisms have a small depth extent, a short strike length will increase the anomaly maximum (case *c* and *d*). For prisms with great depth extent the anomaly decreases when the prism strike length becomes small enough (case *a*). A simple description of the effect of strike length on anomaly profiles thus is impossible. The description becomes still more difficult when one considers profiles across various parts of the prism even if one restricts the consideration to

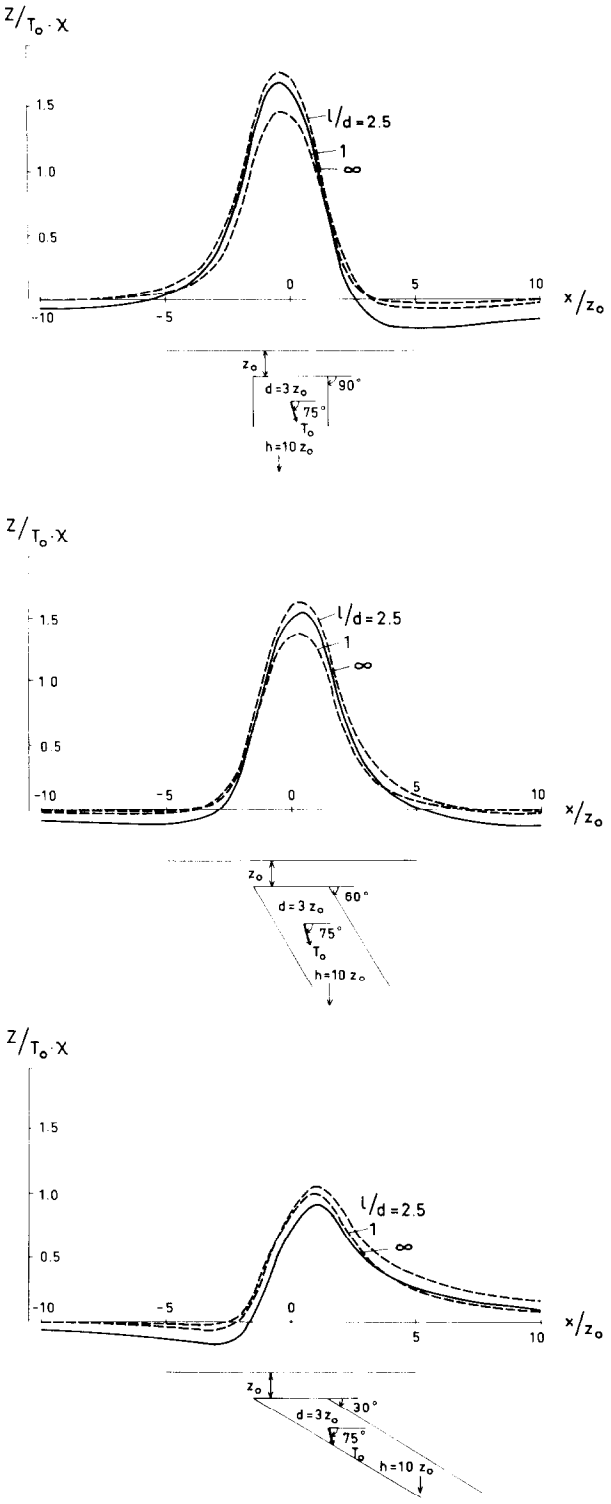

Fig. 3. Dipping prisms of great depth extent. Influence of strike length, l, on center profiles perpendicular to the strike (vertical field component). d = thickness of the prism, h = depth extent of the prism.

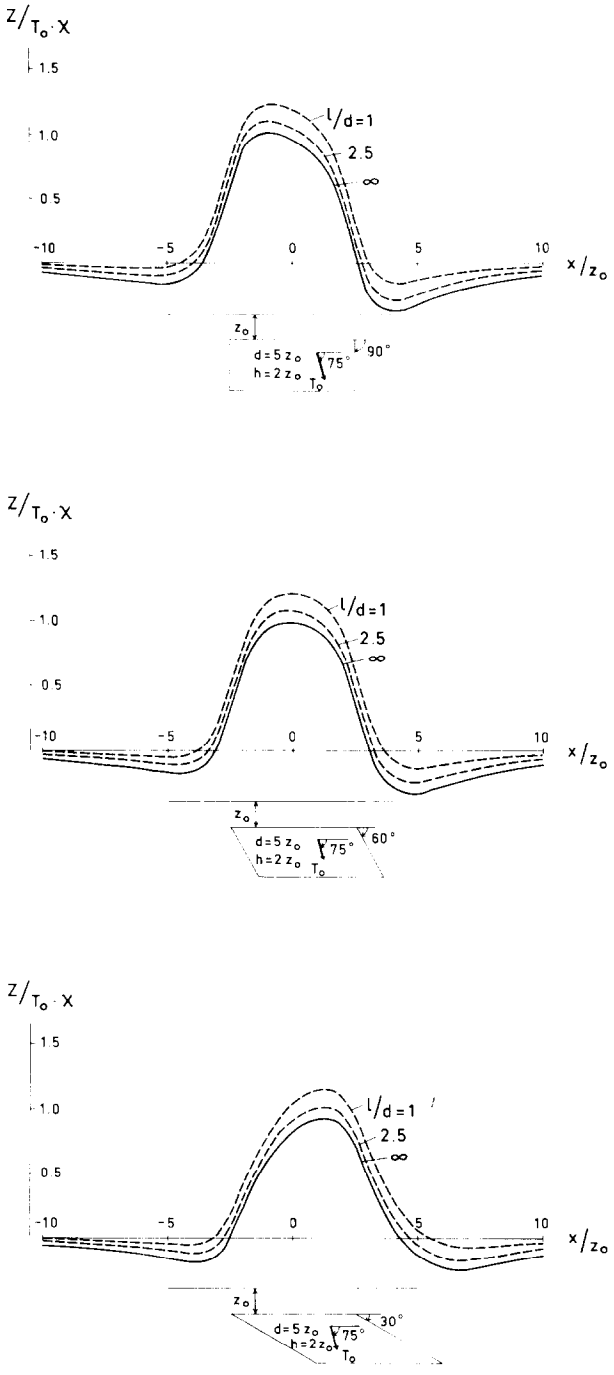

Fig. 4. Dipping prisms of small depth extent. Influence of strike length, l, on center profiles perpendicular to the strike (vertical field component).

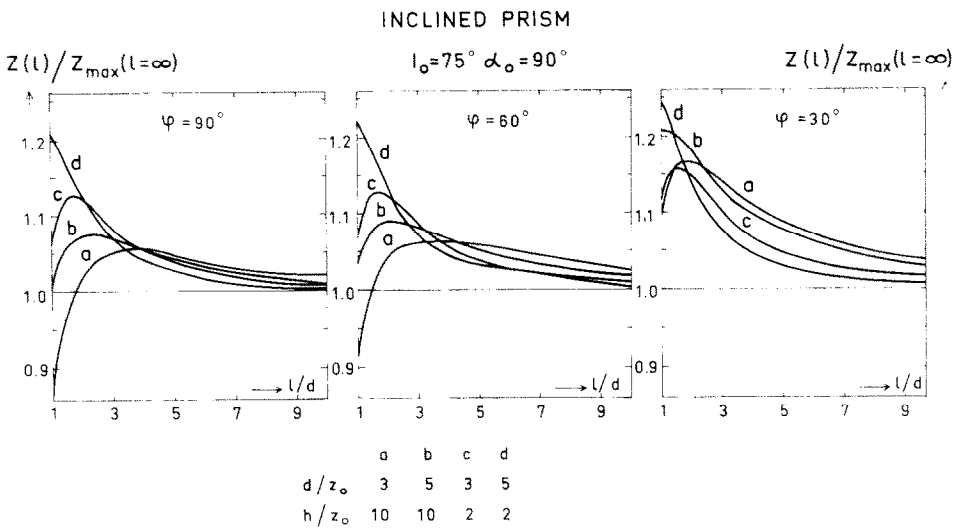

Fig. 5. Influence of strike length on maximum vertical field anomalies of inclined prisms.

perpendicular profiles only (Fig. 6).

Finally Fig. 7–9 show anomaly maps of some prisms with small depth extent, where the effects of dip and different strike directions can be seen. The maps are constructed using a contouring program with linear interpolation (Ketola et al., 1972).

CONCLUSIONS

The expressions of the magnetic field of homogeneously magnetized, dipping prisms are only slightly more complicated than the corresponding vertical prism formulae. The new formulae require only some ten percent more computing time and this should be valuable when attempting computerized interpretation of magnetic anomalies, which are not long in the strike direction.

Some sample profiles perpendicular to the strike of the prism have been calculated. Even these restricted results show, that no simple description of finite strike length on the anomalies or their maximum amplitudes can be given. The most important factors seem to be the dip and the thickness/depth and strike length/thickness ratios.

ACKNOWLEDGEMENTS

The author thanks Dr. M. Ketola and Mr. T. Ahokas of Outokumpu Exploration Department for fruitful discussions and help during the development of the formulae and the calculation tests, and Dr. D.S. Parasnis for valuable comments on the manuscript.

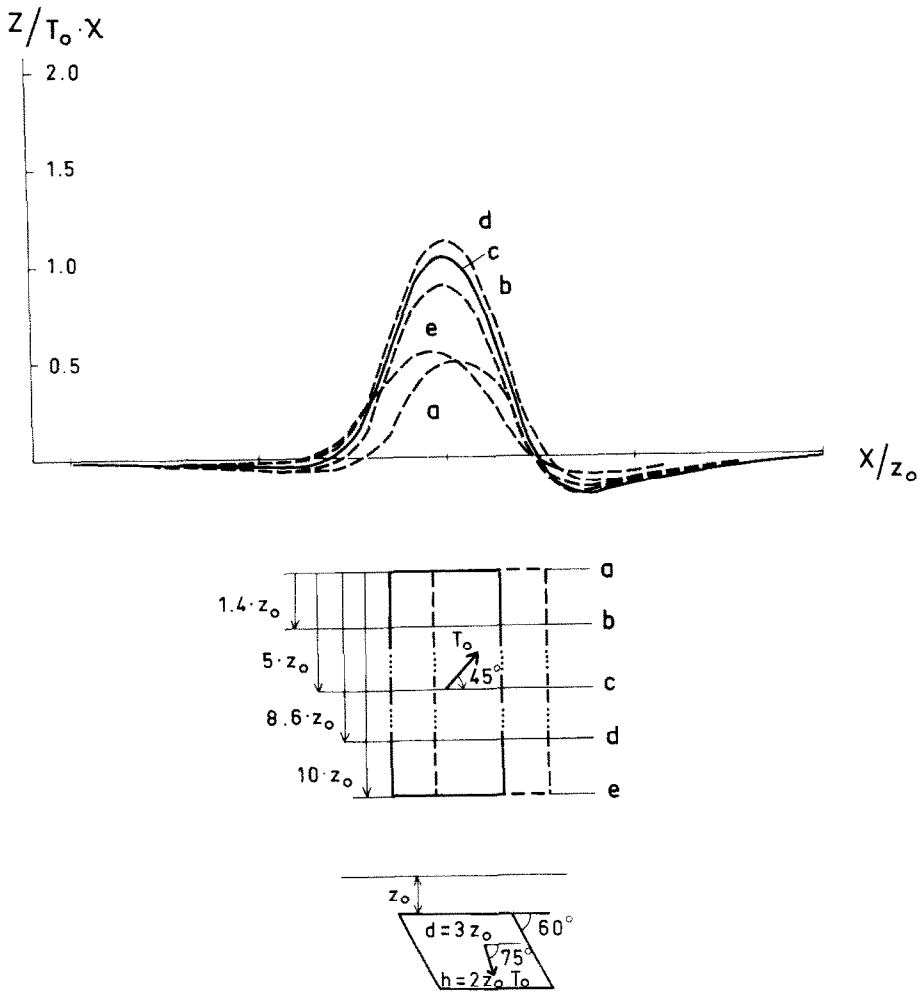

Fig. 6. Total field profiles across various parts of a long, dipping prism of small depth extent. (For anomaly map, see Fig. 9.)

APPENDIX

The factors T_{ij} in eq. 3 are easily identified from the basic integral (eq. 2). They contain following three integrals and their derivatives:

$$T_{1i} = \frac{\partial}{\partial x} I_i$$

$$T_{2i} = \frac{\partial}{\partial y} I_i$$

$$T_{3i} = \frac{\partial}{\partial z} I_i$$

$$I_1 = \int_{\xi_a}^{\xi_b} \int_{a_2}^{b_2} \Big/_{\xi=0}^{\xi=(b_1-a_1)\cdot\sin\phi} \frac{d\zeta \cdot dy_o}{R}$$

$$I_2 = \int_{a_3}^{b_3} dz_o \int_{a_1+(z_o-a_3)\cdot\cot\phi}^{b_1+(z_o-a_3)\cdot\cot\phi} \Big/_{y_o=a_2}^{y_o=b_2} \frac{dx_o}{R}$$

$$I_3 = \int_{a_1}^{b_1} \int_{a_2}^{b_2} \Big/_{z_o=a_3}^{z_o=b_3} \frac{dx_o \cdot dy_o}{R}$$

with: $\xi = (x-a_1)\cdot\sin\phi-(z-a_3)\cdot\cos\phi$

$\zeta = (x-a_1)\cdot\cos\phi+(z-a_3)\cdot\sin\phi$

The integrals can be calculated using the results of standard tables of integrals (Gradshteyn and Ryzhik, 1965). The three important, non-trivial integrals are given in Table II, which also indicates in what factors T_{ij} each of these integrals are needed.

TABLE II

Three important integrals. The numbers in the last column relate to the formulae of Gradshteyn and Ryzhik (1965)

Integral	Result	Needed in	Gradshteyn and Ryzhik (1965)
$\int \frac{dx}{\sqrt{x^2+A}}$	$\ln(x+\sqrt{x^2+A})$	T_{11}, T_{13}, T_{21} T_{23}, T_{31}	2.271.4
$\int \frac{dx}{(x^2+A)\sqrt{x^2+A+B}}$	$\frac{1}{\sqrt{AB}}\cdot\arctan\left[\frac{x\cdot\sqrt{B}}{\sqrt{A(x^2+A+B)}}\right]$	T_{11}, T_{22} T_{31}, T_{33}	2.284
$\int \frac{dx}{\sqrt{Cx^2+Bx+A}}$	$\frac{1}{2\sqrt{c}}\cdot\ln\left[\frac{B}{2\sqrt{c}}+\sqrt{c}\cdot x+\sqrt{Cx^2+Bx+A}\right]$	T_{12}, T_{32}	2.261

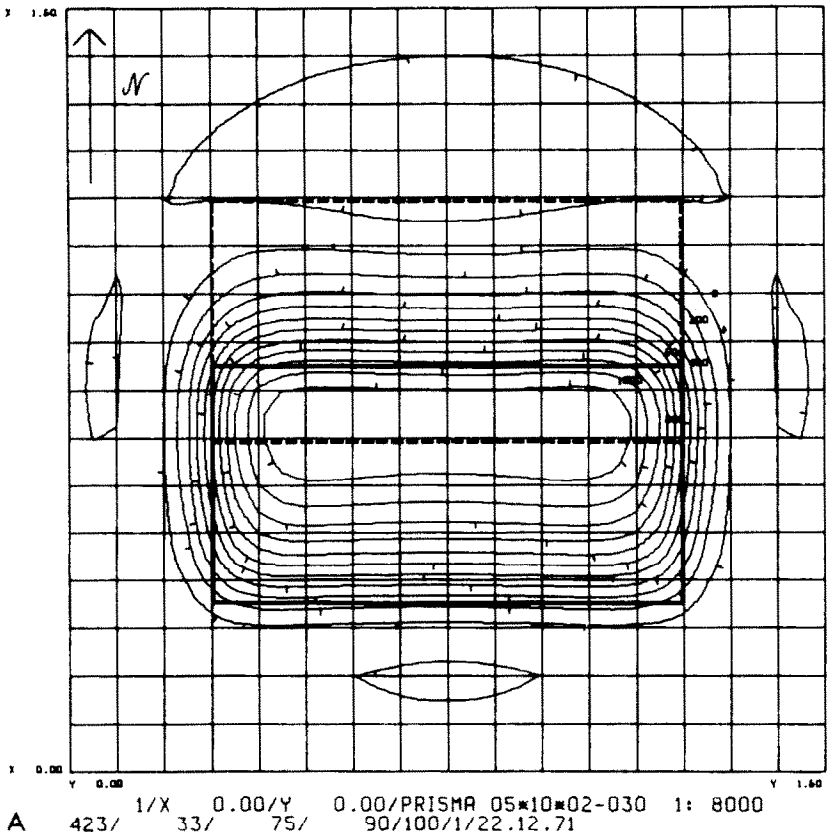

Fig. 7A–C. Vertical field anomaly maps of prisms showing the effect of dip. Codes below each map are as follows: Row 1: No. of map/ vertical coordinate, its value at map origin/ horizontal coordinate, its value at map origin/ model name: thickness * strike * length * depth – dip/scale of original map. Row 2: Field identificator/ no. of points on a profile/ inclination/ prism azimuth/ contour values in γ/ contour value multiplier/ date. The sides of the small squares are equal to the depth to the prism upper surface (= 0.1 map units). Geomagnetic total field = 51,000 γ, apparent susceptibility of the prism = 0.01 c.g.s. units.

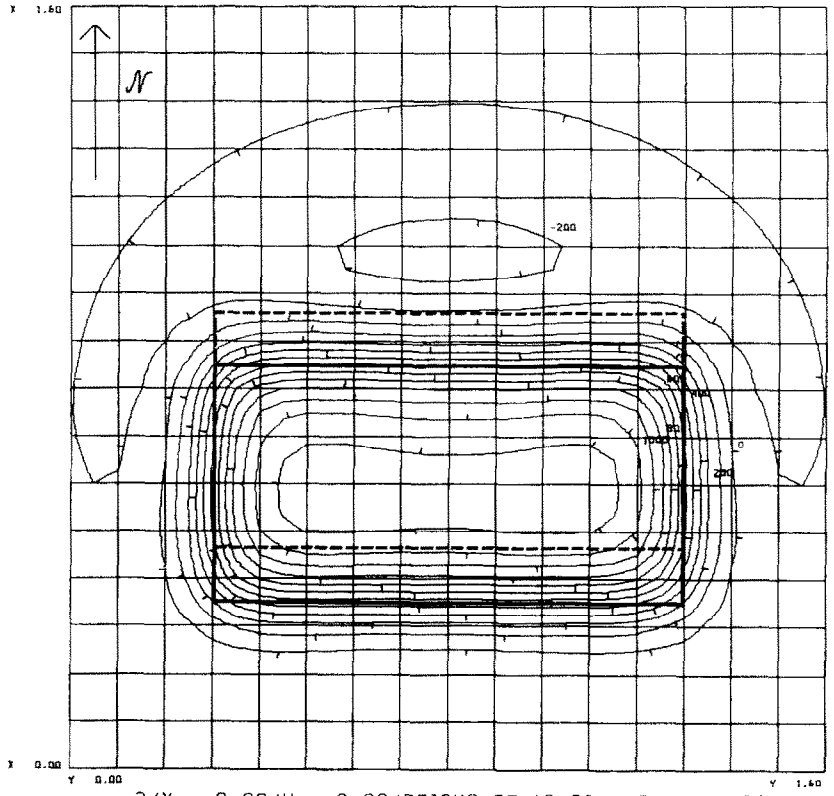

2/X 0.00/Y 0.00/PRISMA 05*10*02-060 1: 8000

B 423/ 33/ 75/ 90/100/1/22.12.71

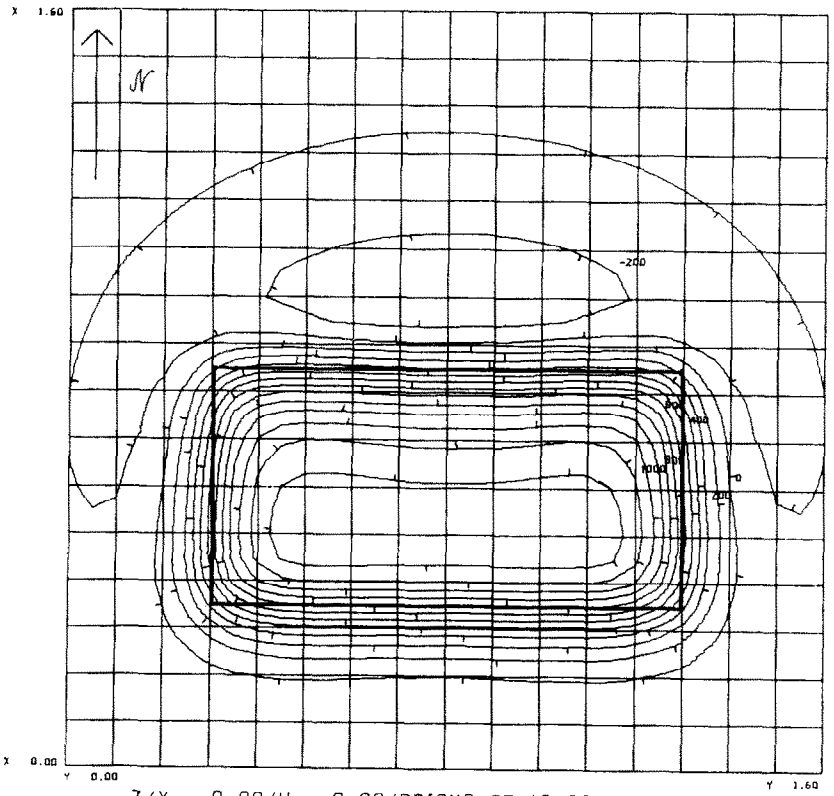

3/X 0.00/Y 0.00/PRISMA 05*10*02-090 1: 8000

C 423/ 33/ 75/ 90/100/1/22.12.71

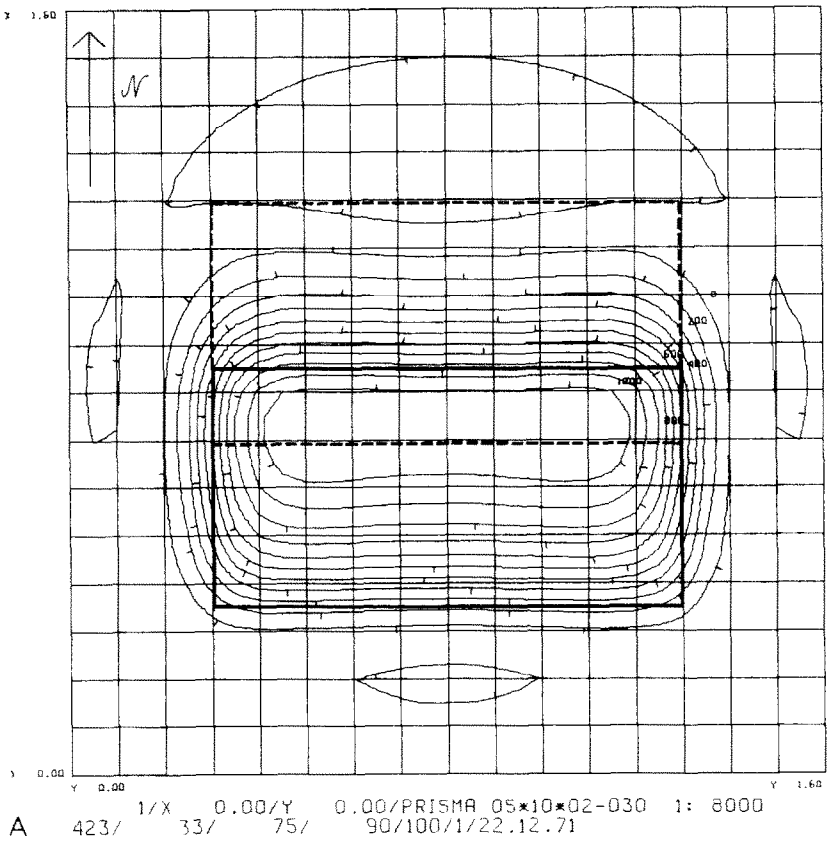

Fig. 8A–C. Vertical field anomaly maps of dipping prisms showing the effect of azimuth. For notations, see Fig. 7.

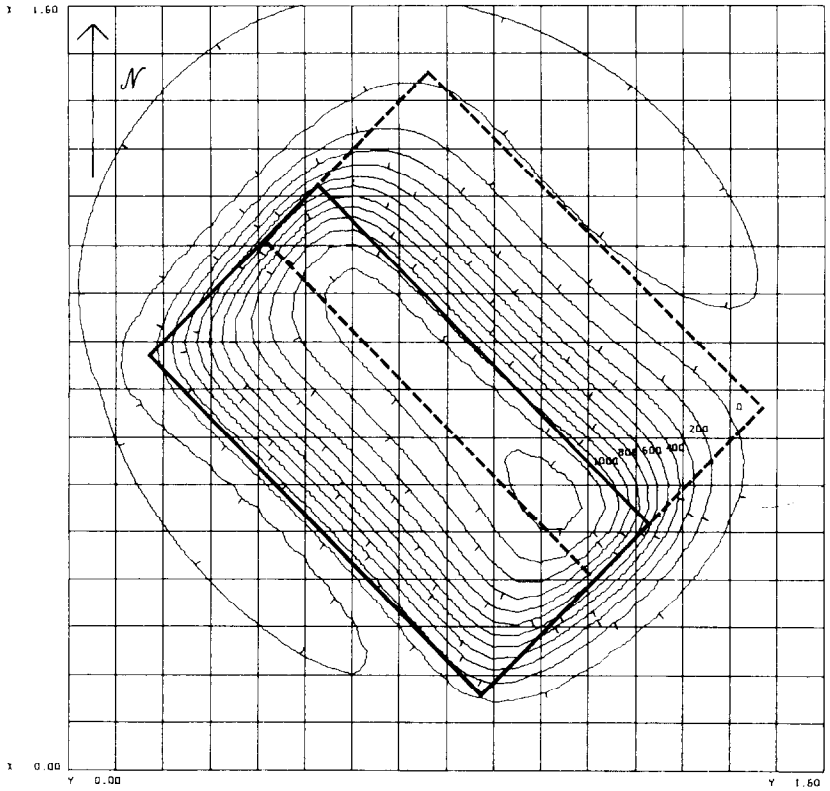

4/X 0.00/Y 0.00/PRISMA 05*10*02-030 1: 8000

B 423/ 33/ 75/ 135/100/1/27.12.71

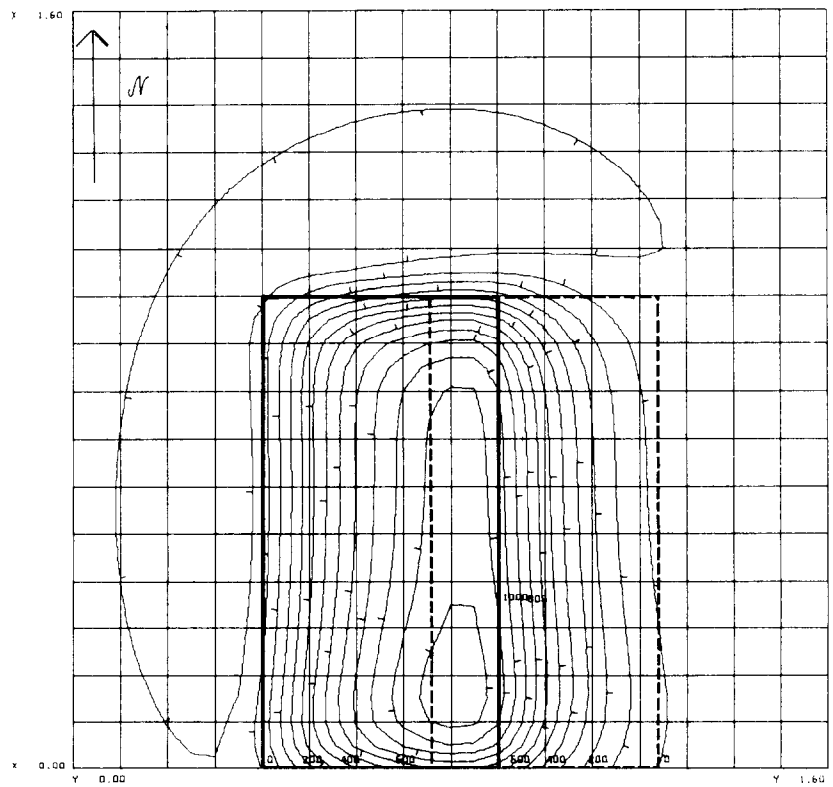

7/X 0.00/Y 0.00/PRISMA 05*10*02-030 1: 8000

C 423/ 33/ 75/ 180/100/1/28.12.71

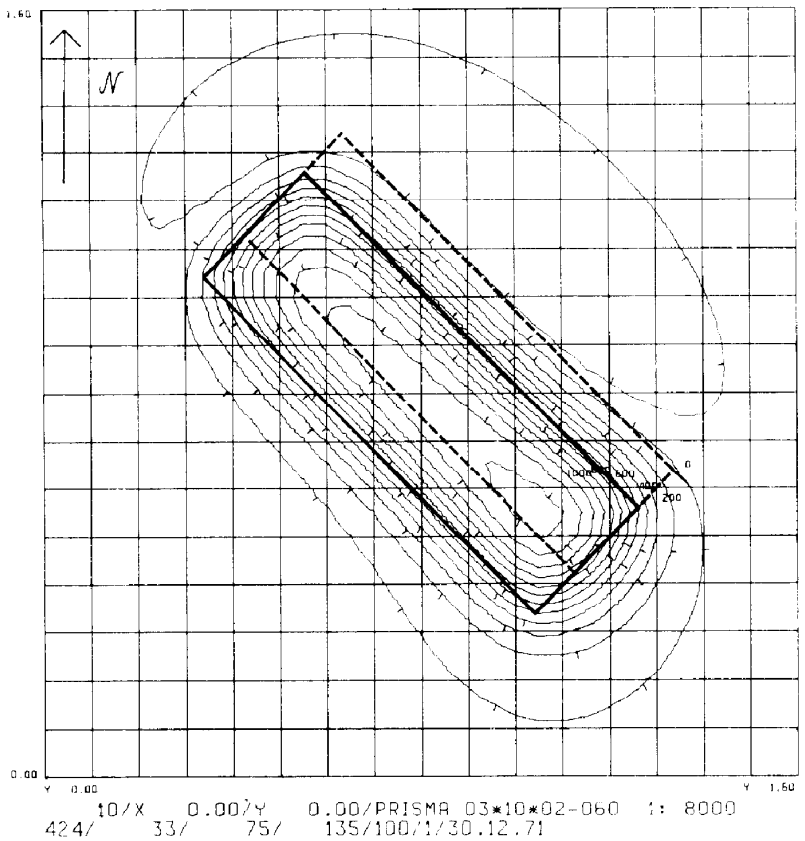

Fig. 9. Total field anomaly map of a long, dipping prism of small depth extent. For notations, see Fig. 7; for corresponding profiles, see Fig. 6.

REFERENCES

Andreasen, G.E. and Zietz, I., 1969. Magnetic fields for a 4×6 prismatic model. *U.S., Geol. Surv., Prof. Pap.*, 666: 219 pp.

Bhattacharyya, B.K., 1964. Magnetic anomalies due to prism-shaped bodies with arbitrary polarization. *Geophysics*, 29: 517–531.

Gay, S.P., Jr., 1963. Standard curves for interpretation of magnetic anomalies over long tabular bodies. *Geophysics*, 28: 161–200.

Gradshteyn, I.S. and Ryzhik, I.M., 1965. Table of integrals, series and products. Academic Press, New York, N.Y., 1086 pp.

Ketola, M., Laurila, M. and Suokonautio, V., 1972. On a digital two-plane rotary field airborne system and its use in conjunction with the magnetic method in Finland. *Geoexploration*, 10: 203–220.

Sharma, P.V., 1966. Rapid computation of magnetic anomalies and demagnetization effects caused by bodies of arbitrary shape. *Geofis. Pura Appl.*, 64: 89–109.

Vacquier, V.W., Steenland, N.C., Henderson, R.G. and Zietz, I., 1951. Interpretation of aeromagnetic maps. *Geol. Soc. Am. Mem.*, 47: 150 pp.